Provided for non-commercial research and education use.
Not for reproduction, distribution or commercial use.

This article appeared in a journal published by Elsevier. The attached copy is furnished to the author for internal non-commercial research and education use, including for instruction at the authors institution and sharing with colleagues.

Other uses, including reproduction and distribution, or selling or licensing copies, or posting to personal, institutional or third party websites are prohibited.

In most cases authors are permitted to post their version of the article (e.g. in Word or Tex form) to their personal website or institutional repository. Authors requiring further information regarding Elsevier's archiving and manuscript policies are encouraged to visit:

http://www.elsevier.com/authorsrights

Author's personal copy

Continental Shelf Research 65 (2013) 97–110

Contents lists available at ScienceDirect

Continental Shelf Research

journal homepage: www.elsevier.com/locate/csr

Research papers

A numerical study of gyres, thermal fronts and seasonal circulation in austral semi-enclosed gulfs

Mariano H. Tonini [a,*], Elbio D. Palma [b], Alberto R. Piola [c]

[a] Instituto Argentino de Oceanografía, CONICET, Bahía Blanca, Argentina
[b] Departamento de Física, Universidad Nacional de Sur and Instituto Argentino de Oceanografía, CONICET, Bahía Blanca, Argentina
[c] Departamento de Oceanografía, Servicio de Hidrografía Naval Argentina, Departamento de Ciencias de las Atmosferas y los Océanos, Universidad de Buenos Aires, Instituto Franco-Argentino Sobre Estudios de Clima y sus Impactos and CONICET, Buenos Aires, Argentina

ARTICLE INFO

Article history:
Received 8 February 2013
Received in revised form
10 June 2013
Accepted 11 June 2013
Available online 18 June 2013

Keywords:
Numerical modeling
Gyres
Thermal fronts
Seasonal circulation

ABSTRACT

This article analyses the results from a high resolution numerical model of the North Patagonian Gulfs (San Matías Gulf, SMG; Nuevo Gulf, NG; and San José Gulf, SJG), a region of the South Western Atlantic Shelf that has long been recognized for its high productivity and biodiversity. The aim of the study is to explore the physical processes that control the mean circulation and its seasonal variability with focus on the generation of recirculation features (gyres) and frontal structures. The numerical results showed that both tidal and wind forcing significantly contribute to delineate the frontal structures and the seasonal circulation in the North Patagonian Gulfs. The overall summer circulation pattern in SMG is dominated by two strong cyclonic subgyres in the northern and southern sectors while NG showed only one gulf-wide cyclonic gyre. The northern subgyre in SMG and the NG gyre are caused by the interaction of the tides and the evolving stratification driven by surface heat and freshwater fluxes. A series of sensitivity experiments showed that the formation and intensity of a summer zonal front in SMG is controlled by the wind-driven advection of cold waters from a homogenized pool generated by intense tidal mixing in the inner continental shelf (east of Valdés Península). From April to August, when winter erodes the stratification, the northern SMG subgyre and the NG gyre spin down and gradually shrink in size. At this time of the year, the western SMG and NG are occupied by an anticyclonic gyre driven by intense westerlies. In contrast, the mean circulation in SJG is dominated year-round by a pair of strong counter-rotating eddies produced by tidal rectification.

© 2013 Elsevier Ltd. All rights reserved.

1. Introduction

The inner continental shelf circulation is strongly influenced by the configuration of the coast and the bottom topography, which can control the exchange of mass and properties with the open ocean and therefore determine the main biological characteristics of the coastal ecosystem. Several studies have linked the distribution of plankton as well as fish larvae and shellfish dispersion to semi-enclosed circulations and the cycles of vertical stratification, whose characteristics are mostly established by the configuration of the coast (e.g. Hill et al., 1997; Horsburgh et al., 2000). Given the strong links between the physical characteristics of the shelf and its biological response, a better understanding of the circulation patterns, associated frontal systems, and their dynamical balance is needed.

The North Patagonian Gulfs (NPG) (Fig. 1) comprise three semi-enclosed gulfs: the San Matias (SMG), Nuevo (NG) and San Jose (SJG) (Fig. 1a and b) and is one of the most productive areas of the Patagonian Shelf ecosystem (Acha et al., 2004). The energy cascades from phytoplankton to higher trophic levels, including major fishing resources like Patagonian anchovy, Argentinean hake, squids and scallops (Lasta and Bremec, 1998; Bogazzi et al., 2005). The coastal areas also present high diversity of birds and mammals (Acha et al., 2004). The high rates of biological activity have been associated with the formation of frontal systems, particularly the Valdés Front (VF, Fig. 1b), and are therefore strongly linked to the shelf dynamics (Carreto et al., 1986; Sabatini and Martos, 2002; Acha et al., 2004; Bogazzi et al., 2005). However, the details of the circulation within the Gulfs, the exchanges between the gulfs and the adjacent shelf, the formation process and dynamics of the frontal systems and their biological impact are still poorly understood.

The NPG region is characterized by large tidal amplitudes (Glorioso and Flather, 1997; Palma et al., 2004a; Moreira et al., 2011), intense westerly winds, particularly in winter (Palma et al.,

* Corresponding author.
E-mail addresses: mtonini@criba.edu.ar, mhtonini@gmail.com (M.H. Tonini).

0278-4343/$ - see front matter © 2013 Elsevier Ltd. All rights reserved.
http://dx.doi.org/10.1016/j.csr.2013.06.011

Author's personal copy

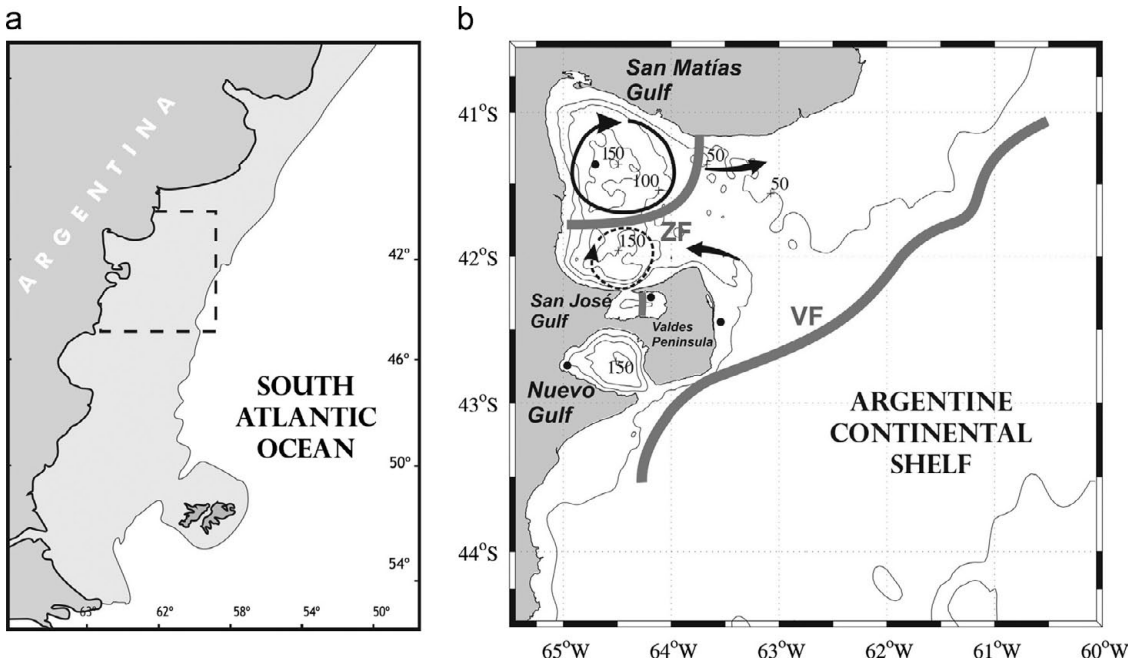

Fig. 1. (a) Location of study area and (b) schematic drawing of the mean flow. The thin lines indicate the 50, 100 and 150 m isobaths and the thick gray lines in b indicate the Valdés (VF) and SMG (ZF) surface fronts, respectively. The black dots indicate the stations analyzed in the model spinup, from south to north, west of Nuevo gulf (NG), east of Valdés Península (VP), San Jose gulf (SJG) and north of San Matías gulf (SMG).

2004b), and significant surface heat and freshwater fluxes (Scasso and Piola, 1988; Rivas and Beier, 1990). The dynamical interplay of these forcings together with the coastal and bottom configurations set up the ocean circulation and lead to the generation of strong fronts and gulf-wide re-circulating patterns (gyres). There are few direct current observations in the shelf area and even fewer inside the Gulfs that are long enough to provide an estimate of the annual mean flow or its seasonal variability (e.g. Framiñan et al., 1991; Rivas, 1997). Most observations are near-shore and the records are masked by high-frequency variability (e.g. Lanfredi et al., 1979; Moreira et al., 2009), inertial and tidal fluctuations, preventing the determination of mean flow patterns in the inner gulfs. For this reason, the mean circulation and their connections with the adjacent continental shelves have been inferred from water mass property distributions and biological indicators (Carreto et al., 1974; Glorioso, 1987; Piola and Scasso, 1988; Rivas and Beier, 1990) and by simplified numerical models (i.e. Barros and Krepper, 1977; Glorioso and Simpson, 1994; Mazio et al., 2004; Moreira et al., 2011).

Piola and Scasso (1988) suggested that the circulation in SMG is characterized by a 30 km radius cyclonic gyre located in the northern half of the gulf. Their study also suggests less defined closed circulation patterns in the southern SMG (Fig. 1b). Scasso and Piola (1988) indicate that SMG presents a salinity maximum relative to the open shelf waters due to an excess evaporation over precipitation of around 100 cm yr^{-1}, which is favored by the relatively higher sea surface temperatures found within the gulf. Based on data collected during two cruises carried out in April and September 1986, Rivas and Beier (1990) suggested that this relative salinity maximum might be generated by the isolation of the gulf waters in northern SMG. They also argued that the southern sector remains colder and fresher by the injection of shelf waters through the mouth (Fig. 1b).

These recirculation patterns may have biological and environmental implications. In the Irish Sea, for example, the gyre circulation contributes to the retention of larvae of Norway Lobster, *Nephrops norvegicus* (Brown et al., 1995; Hill et al., 1996) and of pelagic juvenile fish (Dickey-Collas et al., 1997). Similar circulation patterns could act to retain contaminants in the event of an oil spill (Horsburgh et al., 2000). Similarly, the isolation of the northern SMG in spring–summer may be important in the larval retention and persistence of shellfish population (Amoroso et al., 2011).

Carreto et al. (1974), pointed out that SMG presents two regions with clear differences: the north and west regions filled with "gulf waters" of high temperature and salinity and an intense thermocline in summer; and the south and east regions, filled with shelf waters, characterized by lower temperature and salinity, lack of a seasonal thermocline and high concentrations of nitrates. Based on the analysis of hydrographic data Piola and Scasso (1988) indicate that these regions are separated by a zonal thermohaline front (ZF) situated near 41° 50′ S and suggested that the cold-fresh water found south of the front enters the gulf through the southern portion of the mouth (Fig. 1b). Satellite data confirm the existence of this front (Gagliardini and Rivas, 2004) and suggest that intense exchanges with SJG could influence the thermohaline structure of the southern SMG and the formation of the ZF (Amoroso and Gagliardini, 2010).

More recent research based on the analysis of barotropic (i.e. constant density) numerical models of ~1 km of spatial resolution indicates that tidal forcing plays a dominant role in shaping the annual mean circulation (Tonini and Palma, 2011). Presumably the barotropic simulation is representative of the winter season, when the water column is well mixed. The main goal of the present study is to increase our physical understanding of the NPG dynamics by exploring the effects of stratification on the mean three dimensional circulations with focus on the formation, interaction and seasonal variability of gulf-wide recirculation features and formation mechanisms of the frontal structures. The use of a numerical model allows us to reduce the complexity of the problem by separately analyzing the effects of various interacting factors. An improved understanding of the behavior (dynamics) of the circulation and its variability is essential to understand the spawning cycle, feeding and reproduction patterns of a variety of species which use these ecosystems. After this Introduction, Section 2 describes the numerical model and its physical configuration. In Section 3 we present and analyze the model results and in Section 4 the summary and conclusions are presented.

Author's personal copy

2. Ocean model

The numerical model used in this study is the Regional Ocean Modeling System (ROMS). ROMS is a free-surface, terrain-following, primitive equations ocean model widely used for a diverse range of applications (e.g., Haidvogel et al., 2000; Marchesiello et al., 2003). The algorithms that comprise the ROMS computational kernel are described in detail in Shchepetkin and McWilliams (2005). In the vertical, the primitive equations are discretized over variable topography using stretched terrain-following coordinates. The stretched coordinates allow increased resolution in areas of interest, such as surface and bottom boundary layers. In the horizontal, the primitive equations are evaluated using orthogonal curvilinear coordinates on a staggered Arakawa C-grid. The vertical mixing parameterization in ROMS can be set either with local or nonlocal turbulent closure schemes. In this study we used a local scheme originally developed by Mellor and Yamada (1982).

2.1. Model setup

The computational grid has 271 nodes in alongshore (N–S) and 241 nodes in a cross-shore (W–E) direction and extends from 40° to 44° S and from 60° to 65° W (Fig. 1b). The spatial resolution of the grid is variable, with maximum resolution (~1 km) in the gulfs. In the vertical the model equations are discretized in 20 sigma levels, with higher vertical resolution at the top and bottom layers. The bathymetry is based on digitized nautical charts. The model has three open boundaries (Fig. 1a) where a combination of radiation and advection conditions is used (Marchesiello, et al., 2001). At these lateral open boundaries we imposed tidal amplitudes and phases of six constituents (M_2, S_2, N_2, O_1, M_1 and P_1) interpolated from a global tidal model (TPOX6, Egbert et al., 1994). At the sea surface we forced the model with the monthly mean climatological wind stress (τ^w) from the SCOW 8-year Quikscat climatology of ¼ degree spatial resolution (Risien and Chelton, 2008) and heat and freshwater fluxes. The net downward heat flux (Q) is calculated according to the formulation of Barnier (1998)

$$Q = Q_C + D_q(SST_m - SST_c) \quad (1)$$

where Q_C is the monthly mean climatological net heat flux (including short wave, long wave, latent and sensible heat components), D_q is a monthly mean climatological heat flux sensitivity, SST_m is the model-derived sea surface temperature (SST) and SST_c is the monthly mean climatological SST. Q_C was determined using a simplified model proposed by Rivas and Piola (2002)

$$Q_C = Q_o \cos[\omega(t - t_0)] \quad (2)$$

with $Q_o = 144.3\ W/m^2$, $\omega = 2\pi/360$; and $t_0 = -18$ days. D_q, SST_c and the net monthly mean climatological freshwater fluxes (E−P, evaporation minus precipitation) were obtained from COADS (daSilva et al., 1994).The climatological fields (τ^w, D_q, SST_c and E −P) are interpolated onto the model grid, and for each time step in the model integration the instantaneous values are calculated by time-intepolating the climatological fields between the two bracketing months. Each month is assumed to consist of 30 days; thus a model year consists of 360 days. Near coastal winds (< 25 km from shore) were obtained from the first available oceanic record and extrapolated towards land using a five-point laplacian filter. Fig. 2 shows the model's wind stress for January (austral summer) and July (austral winter). Depending on the experiment design, the model was initialized either with constant density (NOHEAT experiment) or with annual mean and area averaged (horizontally uniform) vertical profiles of temperature and salinity extracted from Conkright et al. (2002) (i.e., in the benchmark experiment hereafter referred to as BENCH) and run for four years (Table 1 lists the characteristics of the numerical experiments described in the text).

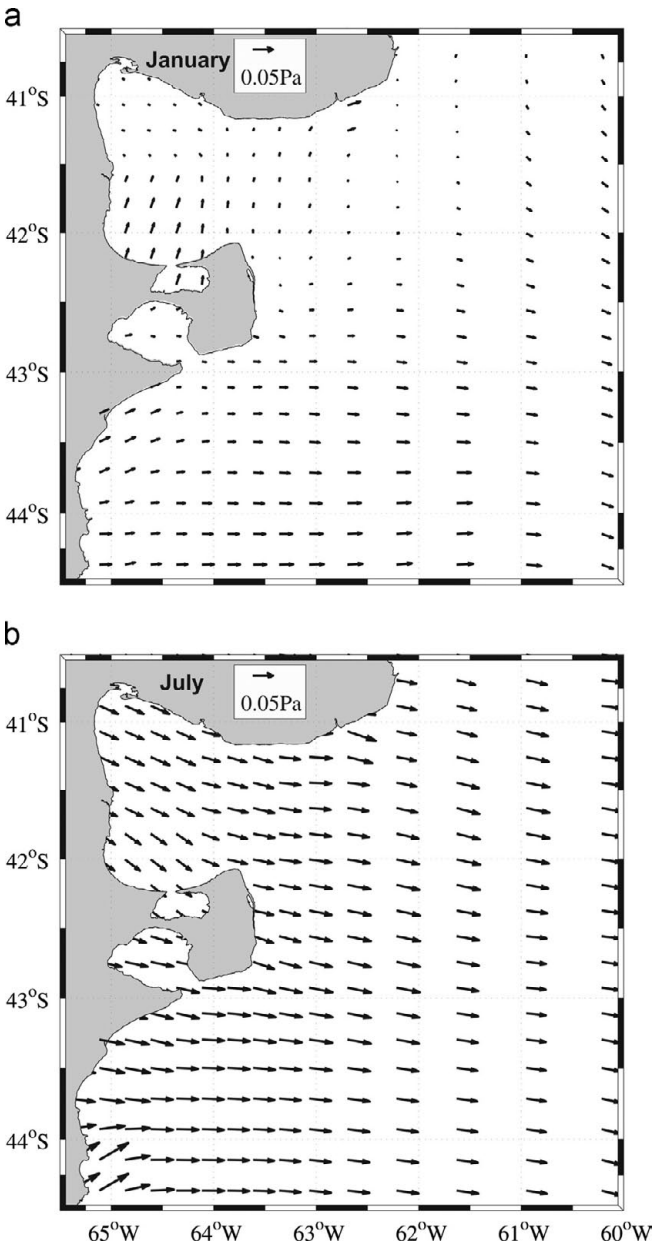

Fig. 2. Sea surface climatological wind stress interpolated onto the model grid. Vectors indicate direction and magnitude of the wind stress [Pa]. (a) January (summer) and (b) July (winter).

Fig. 3 shows the four-year time series of SST and sea surface salinity (SSS) at four selected grid points (indicated in Fig. 1b) of the model domain from the BENCH experiment. The seasonal cycle has been clearly established both in SST and SSS. The model ocean responds rapidly in SST but it took more than two years to reach an equilibrium state in SSS. The year-four model results are thus employed to analyze the simulated circulation in the study region.

3. Results and discussion

3.1. Non-stratified solution

To isolate the effect of stratification on the circulation we have performed a first experiment (NOHEAT, Table 1) forced with tides and winds but without initial vertical variations of density and no surface heat and salt fluxes. The tidally driven response can be characterized by the amplitude and phase of the principal

Author's personal copy

Table 1
General description of the numerical experiments.

Experiment	Heat flux	Wind	Tide	SJG–SMG	Remarks
NOHEAT	No	SCOW	Yes	Connected	Non-stratified experiment
BENCH	COADS	SCOW	Yes	Connected	Stratified experiment (Benchmark)
NOTIDE	COADS	SCOW	No	Connected	No tidal forcing at open lateral boundaries
NOSJG	COADS	SCOW	Yes	Not connected	The mouth of SJG is closed
NOWIND	COADS	No	Yes	Connected	No wind forcing at the surface
05WIND	COADS	0.5 SCOW	Yes	Connected	half magnitude of wind stress
2WIND	COADS	2 SCOW	Yes	Connected	Double magnitude of wind stress

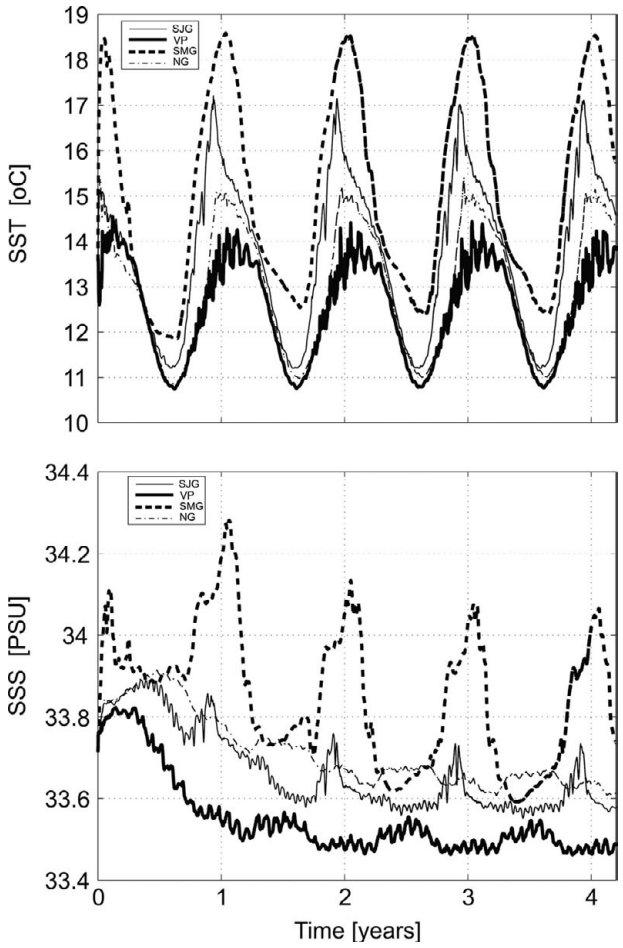

Fig. 3. Numerical model spin-up analyzed in four stations of the computational domain (Fig. 1b). (a) Time evolution of the sea surface temperature and (b) Time evolution of the sea surface Salinity.

harmonic (M_2) and the tidal dissipation rate (Fig. 4). The tidal signal propagates from the southwest as a Kelvin wave and amplifies after entering the SMG (Fig. 4a), dissipating much of its energy at the mouth and northeast of Valdés Península (Fig. 4b). There is an amphidromic point located at 41°30′S, 61°W (Fig. 4a) which has been reported in previous simulations (Palma et al., 2004a; Moreira et al., 2011). Inside NG and SJG the tidal amplitude presents small spatial variations with the maximum being larger at SJG (~3 m). The zones of higher energy dissipation rate (Fig. 4b) denote intense vertical mixing and are correlated with the location of the thermal fronts detected by satellite imagery (Glorioso, 1987; Romero et al., 2006). The total area-integrated energy dissipation attains 12.3 GW with local maxima larger than 7.4 W/m^2 concentrated NE of Valdés Península (Fig. 4b).

Since in January the wind stress is relatively weak (Fig. 2a), the mean (non-stratified) summer circulation is dominated by residual tidal currents (Tonini and Palma, 2011). The vertical integrated stream function shows that the nonlinear interaction between the tidal circulation and the bottom topography leads to the formation of several robust residual circulation patterns (Fig. 5a and b). Other studies based on residual vorticity (Zimmerman, 1981; Robinson, 1983) classified the residual gyres (hereafter referred to as eddies because of their small dimensions) according to their geomorphological origin: basin eddies, headlands (coastal) eddies and topographical (bathymetric) eddies. Based on this classification, NOHEAT presents basin scale gyres at NG and SMG, and bathymetric induced vortices at the mouths of SJG and NG (Fig. 5b). Further details and analysis on the tidal and wind-forced barotropic response are given in Tonini and Palma (2011).

3.2. Stratified solutions

Fig. 5c shows the mean January circulation for BENCH. The most relevant differences observed between NOHEAT and BENCH are the generation of robust cyclonic circulations in SMG and NG, and a reduced exchange between SMG and the open shelf waters (Fig. 5a and c). As we will show later, these differences are due to the interaction between tidal forcing and the development of the vertical stratification induced by the relatively large net summer heat fluxes. The general cyclonic circulation inside SMG is characterized by two re-circulating subgyres: one gyre centered in the northern portion of the gulf, around 41° 20′ S 64° 30′ W and another gyre located around 42°S–64° 30′ W (Fig. 5c). Although the southern gyre is of smaller size, both carry similar transports (0.16 Sv, 1 Sv = 1.10^6 m^3 s^{-1}). A similar circulation pattern in the north has been suggested by Piola and Scasso (1988) using synoptic hydrographic data. The same study suggested a less defined cyclonic closed circulation pattern in the south, but the data was too sparse at that location. In the model, the southern gyre appears to be mainly controlled by topographic rectification of tidal currents (Fig. 5a) but the intensity of the circulation is increased by the stratification (Fig. 5c). The inclusion of stratification and heat fluxes also intensifies the NG gyre (Fig. 5c). NG has only one deep basin and therefore only one cyclonic gyre is formed that spans the entire gulf. Unlike SMG, the circulation near the gulf's mouth is similar to NOHEAT and dominated by tidal residual currents (Fig. 5a and c). The SJG circulation is relatively insensitive to the inclusion of stratification and surface heat flux forcing. The dynamics in both the mouth and the interior is dominated by a pair of counter-rotating eddies generated by tidal residual currents near the mouth and extending towards the interior (Fig. 5b and c).

To better display the role of tidal forcing on shaping the January mean circulation, we performed another experiment (NOTIDE) initialized and forced at the surface as BENCH but without tidal forcing at the lateral boundaries. The resulting stream function shows completely different circulation patterns (Fig. 5d), with weak gyres in the SMG and NG interior and the absence of the SJG dipole. Note also that the feeble SMG northern gyre is anticyclonic. This experiment denotes the predominant role that the tide plays on shaping the depth-mean circulation of the region. We will

Author's personal copy

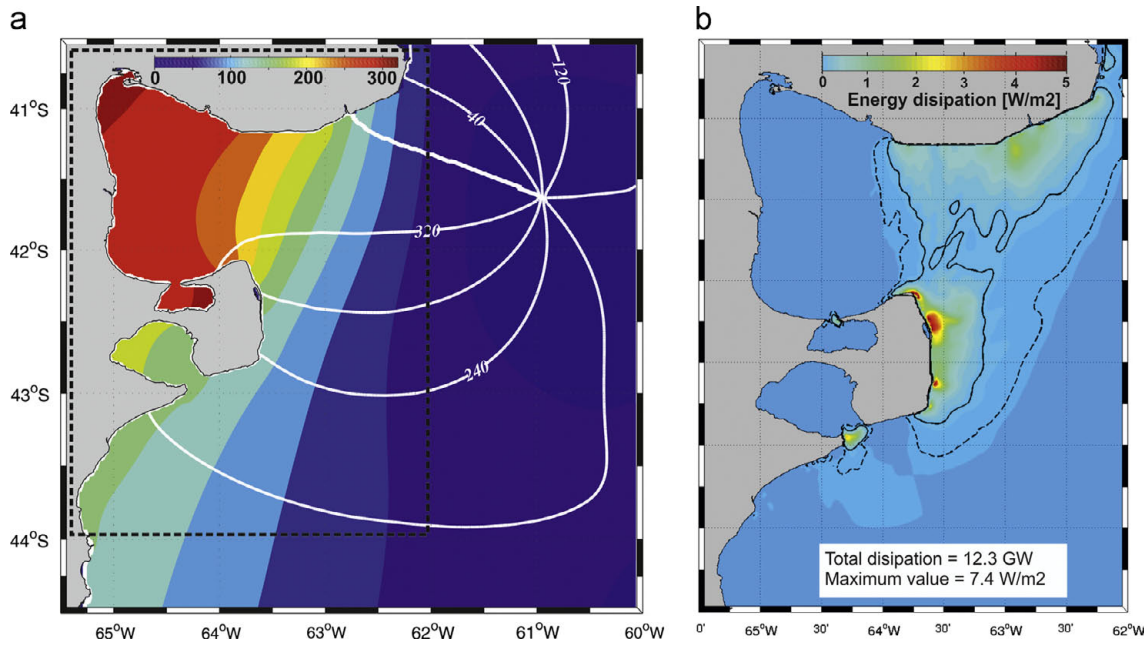

Fig. 4. Barotropic model (NOHEAT) results. (a) Cotidal (white lines) and corange contours (CI = 30 cm and 40°) for the M_2 component. Dotted black lines indicate the area shown in b and (b) tidal energy dissipation in W/m^2. The solid and dotted black lines indicate the 0.25 and 0.1 W/m^2 respectively.

return to this experiment in the analysis of the SMG ZF formation mechanisms (Section 3.4).

3.3. Gyre generation

The model results indicate that the formation of cyclonic gyres (north of SMG and in NG) involves the interaction of vertical stratification, bottom topography, and tides. In winter, the combined effect of vertical mixing induced by the strong westerlies and the negative surface heat fluxes completely mix the water column (Scasso and Piola, 1988). The subsequent increase of heat flux into the ocean in spring–summer induces vertical stratification thus limiting vertical mixing. In turn, the tidal fronts formed at the mouths of SMG and NG in summer (e.g. Rivas and Pisoni, 2010) contribute to isolate the waters within the gulfs. The combination of these processes generate cold and dense water domes remnant from previous winters that are retained in the deeper layers and are blocked by the steep depressions of bottom topography inside the gulfs year-round (Fig. 6a and b).

Hill (1996) showed that domes of dense deep water in shelf seas can be expected to induce significant baroclinic circulations. Although many geostrophic flow states can support a bottom dome structure, cyclonic circulation develops in the upper layers over a stagnant bottom layer. Using a two-layer quasi-geostrophic model Hill (1996) demonstrated that due to the higher bottom friction induced in macrotidal shelf seas, the bottom layer will spin down to rest over a time-scale of a few days, and that, due to layer coupling through vortex stretching/compression, will concentrate the cyclonic flow in the surface layer. Hill's theory was applied to the western Irish Sea summer cyclonic gyre and verified using in-situ data, satellite tracked free drifting buoys and numerical models (Hill et al., 1997; Horsburgh et al., 2000). A similar mechanism can explain the intensification of SMG and NG summer cyclonic gyres (Fig. 5c).

Given that the vertical density structure plays a prominent role in the gyre's intensification in summer, we compare the model vertical density structures (recall the model was initialized with climatological area averaged temperature profiles) with the few available observations. The modeled vertical density distribution along section A (Fig. 6a) shows a strong pycnocline at ~20 m depth. The waters beneath the seasonal pycnocline present a clear doming, with denser waters over the deepest part of the gulf and isopycnals deepening around the edges of the gyre. Near the SMG mouth, the isopycnals deepen sharply in response to the intense vertical mixing induced by the tides at that location (Fig. 4b). The overall density structure displayed by the model in the central part of the section (black rectangle, Fig. 6a) resembles the structure displayed by a CTD section collected in December 1987 (Fig. 6b). Note the 20–50 m deepening of the 26 kg/m^3 isopycnal from the gyre center towards the edges (Fig. 6b). This dome-like shape of the density field also resembles the topography of the 14 °C isotherm observed in April 1977, which deepens from ~50 m in the gyre center to about 80 m around the edges, (Piola and Scasso, 1988). Thus, the near-bottom vertical density structure combined with strong tidal-generated bottom friction appear to be the main elements leading to the summer intensification of the cyclonic circulation.

To quantify the impact of heat fluxes and tidal mixing strength on the model vertical stratification, we analyzed the January potential energy anomaly (PEA). Following Simpson (1981), the PEA is defined as

$$\phi = \frac{1}{h}\int_{-h}^{0}(\overline{\rho}-\rho)g.z.dz; \tag{3}$$

with

$$\overline{\rho} = \frac{1}{h}\int_{-h}^{0}\rho.dz$$

where h is the total depth, ρ the local density, $\overline{\rho}$ the mean density, g is gravity acceleration and z is the vertical coordinate. The model's PEA distribution clearly displays the difference between well mixed and stratified waters, which determine the location of thermal fronts previously detected from remote sensing data, such as Valdés Front (VF) located southeast of Valdés Península and extending in a SW–NE direction (Fig. 6c and d). The PEA distribution also displays a stratification increase in the SMG interior, while the water column is well mixed east of the mouth. In agreement with previous studies (Carreto et al., 1974; Piola and Scasso, 1988) SMG presents two clearly distinct regions: stratified in the north and relatively well-mixed in the south, with a

Author's personal copy

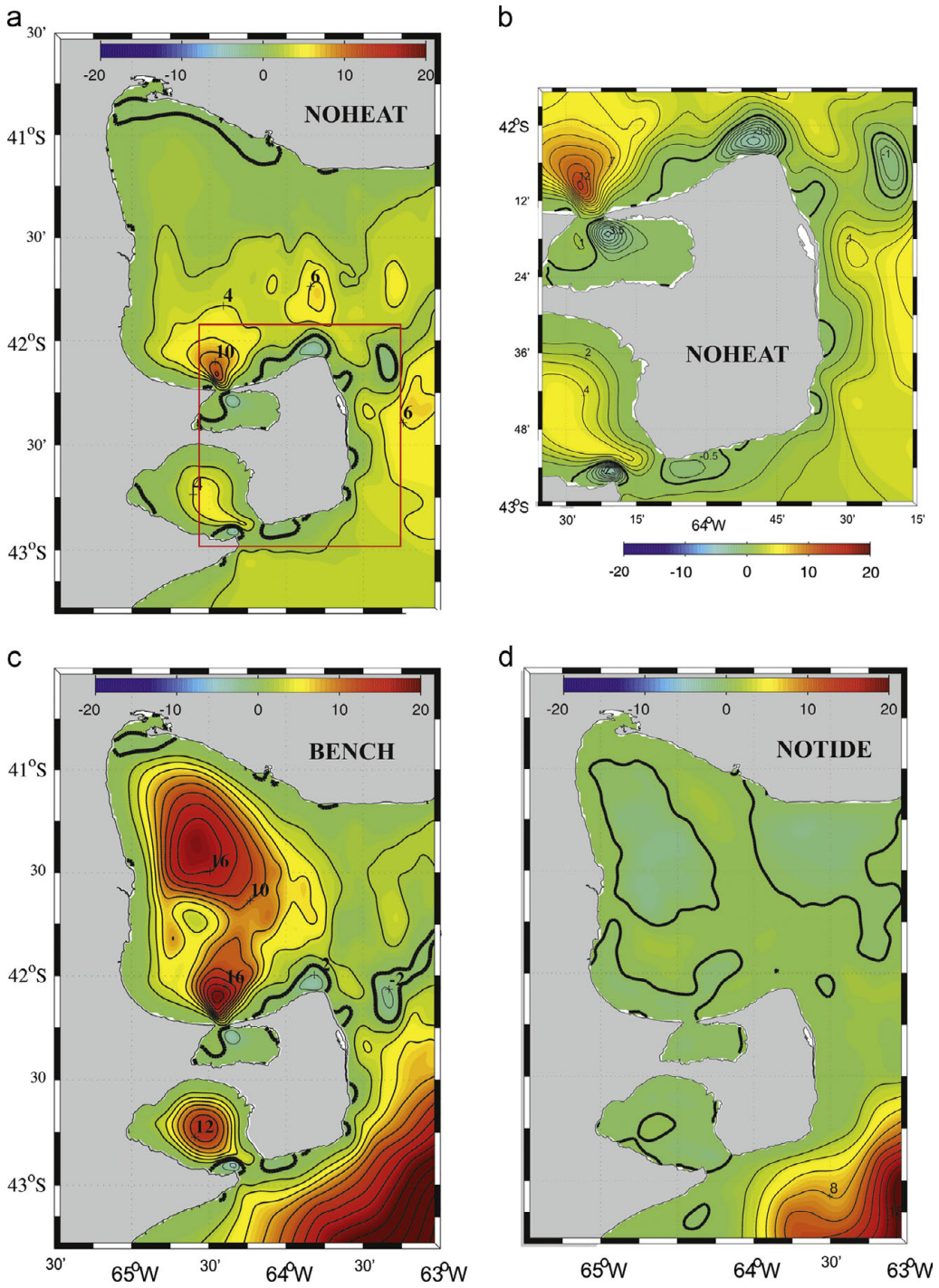

Fig. 5. Vertically integrated stream function for January (austral summer, CI = 2 x 10^4 m^3/s) derived from the non-stratified (a and b, NOHEAT) and stratified (c, BENCH and d, NOTIDE) experiments. Thick red lines in a indicate the area shown in b. The CI in (b) is 1 x 10^4 m^3/s and 5 x 10^3 m^3/s for positive and negative values, respectively. Thick black lines indicate the zero contour. (For interpretation of the references to color in this figure legend, the reader is referred to the web version of this article.)

transition associated with the ZF located near 41°30′S. The PEA reaches 70 J/m^3 in the northern gyre center while decreases to ~35 J/m^3 further south (Fig. 6c). These values are similar to those calculated by Hill et al. (1997) in the Irish Sea gyre, where oceanographic conditions are comparable. Though NG presents lower overall PEA its center displays relatively high PEA (~30 J/m^3) compared to the gyre periphery. Southeast of the VF the PEA is much higher (> 60 J/m^3) because tidal mixing is not strong enough to overcome the summer stratification in the mid shelf region (see Bianchi et al., 2009). The average January 2011 SST from satellite data (Fig. 6d) shows a clear correlation between the surface thermal fronts (ZF and VF) and the stratification areas delineated by the model's PEA. The satellite data was obtained from the G1SST product, a daily global sea surface temperature data set at 1 km by the JPL Our Ocean Portal (ROMS group, http://ourocean.jpl.nasa.gov/SST/). The satellite SST also displays the maximum north of SMG (19 °C) and minima in well mixed areas such as the mouth of SJG, NG and East of Valdés Península (Fig. 6d).

The summer SST distribution and frontal patterns in BENCH are in overall agreement with high resolution satellite SSTs (Figs. 6d and 7a). In BENCH the SMG is divided in two regions north and south of 41° 30′ S (Fig. 7a). In the north surface waters are warm

Author's personal copy

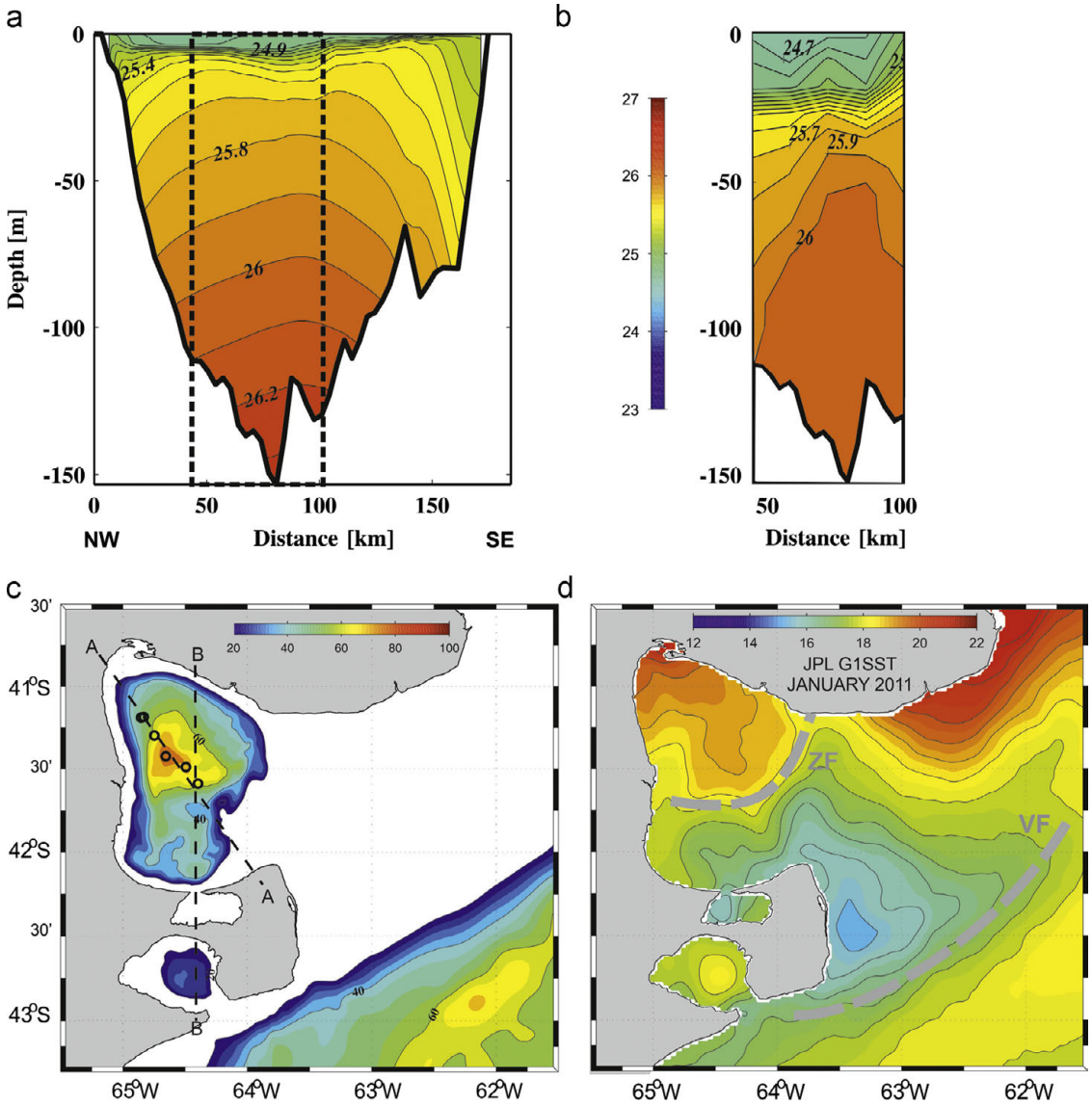

Fig. 6. Vertical density (σ_θ, in kg m^{-3}) sections along line A derived from the January (austral summer) simulation (BENCH, a) and from observations collected in December 1987 (b). The section locations are indicated by the dashed lines in c. (c) Potential Energy Anomaly (PEA, in J/m^3) distribution from the baroclinic simulation (BENCH) in summer. The black circles indicate the stations used to construct the vertical section shown in b. Monthly mean (January 2011) Sea surface temperature (CI = 1 °C) from JPL-G1SST, 1 km spatial resolution (d). The gray dashed lines in d indicate the Valdés Front (VF) and the SMG Zonal Front (ZF).

(> 18.5 °C) and saline (> 34.2, Fig. 3b), where the surface currents delineate the northern cyclonic gyre while in the south, SSTs are lower (15 °C), less saline (33.5, not shown) and surface currents are stronger and suggest the input of shelf waters towards the gulf interior (Fig. 7a). Similar temperature and salinity distributions have been previously described by Carreto et al. (1974) based on hydrographic data. Although the model displays a surface temperature range larger than satellite observations, both distributions present cold regions along the mouths of SMG and NG and west of VF. Given that the model is forced with climatological wind stress and a proxy of long-term averaged heat fluxes the agreement between model and observations is quite good. The model SST in NG is nearly homogeneous (~16 °C), except for a tongue of cold water that extends westward from the mouth along the south coast. This feature is more apparent in the model than in the satellite observations (Figs. 6d and 7a). However, daily satellite derived SST distributions also clearly depict cold water tongues along the south coast of NG (e.g. Amoroso and Gagliardini, 2010, their figure 2a). The small spatial dimensions of SJG and its shallower waters, lead to a reduced influence of stratification compared to tidal forcing. A meridional front in SJG has been detected using daily high resolution (~1 km) satellite data (Amoroso and Gagliardini, 2010). Although this front is not well-defined in the model SST distribution, both, model and observations show that the west part of the gulf is slightly colder than the eastern region (Fig. 7a). This zonal temperature contrast is probably associated with the asymmetry in the location of the gulf's mouth, which leads to higher tidal mixing and homogenization in the west.

3.4. SMG zonal front formation mechanisms

While in the open shelf the net surface heat flux is partially balanced by northeastward advection of cold water (Rivas and Frank Langer, 1996) the isolation of the northern SMG by the spring–summer cyclonic circulation increases its temperature beyond shelf values. In turn, this increase in SST augments the evaporation compared to open shelf waters causing an increase in surface salinity (Scasso and Piola, 1988). Given that the surface heat flux is approximately uniform over the entire region, the

Author's personal copy

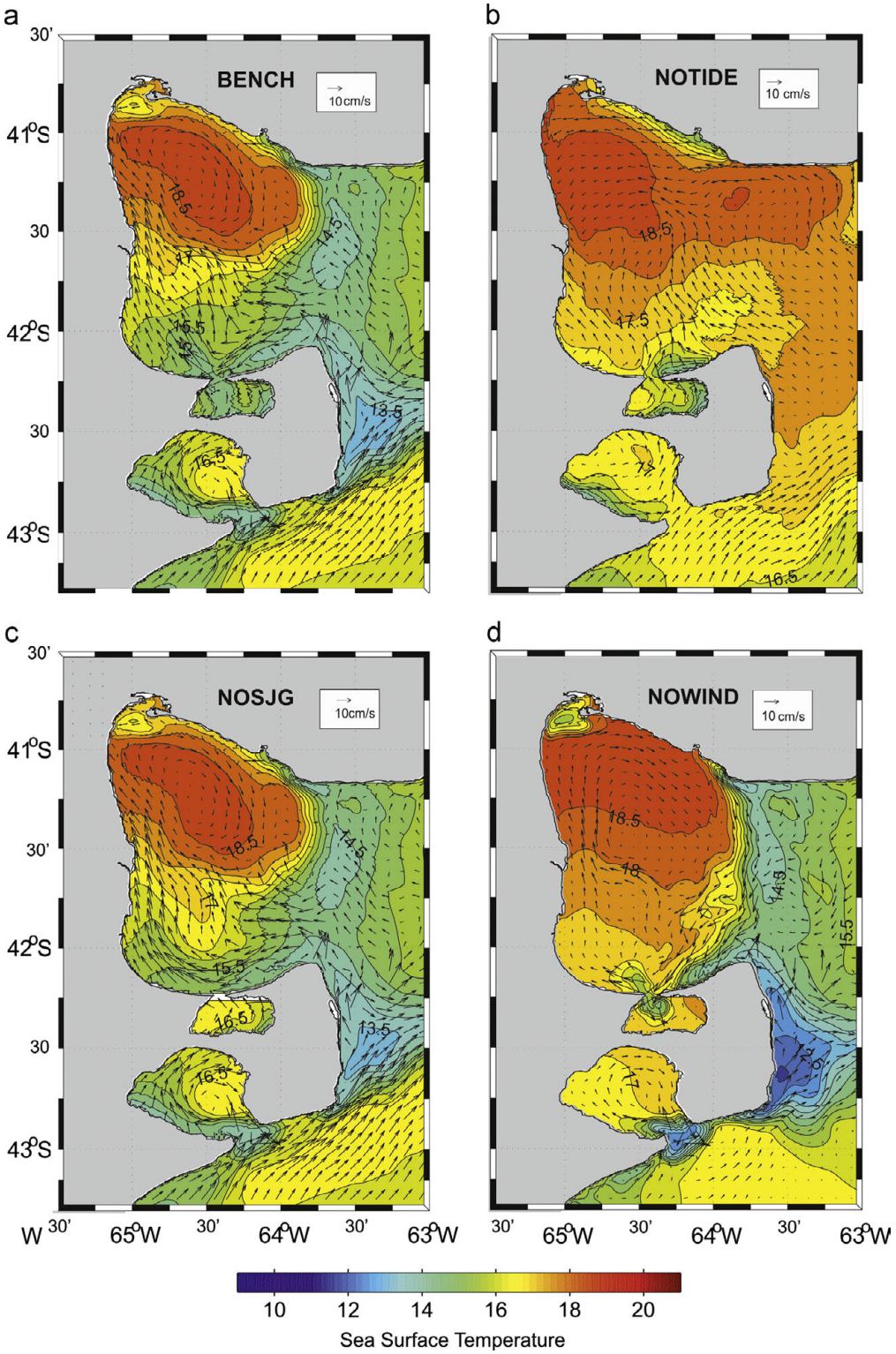

Fig. 7. January (austral summer) sea surface temperature (CI = 0.5° C) and surface velocity vectors (a) Benchmark experiment (BENCH), (b) no tidal forcing at lateral boundaries (NOTIDE), (c) no connection between SMG and SJG (NOSJG) and (d) no wind stress (NOWIND).

meridional SST difference observed in summer at SMG (Fig. 7a) is possibly due to horizontal advection of colder waters into the southern sector. The colder waters may be associated with different physical mechanisms: (i) waters from the adjacent shelf (e.g. east of Valdés Península) carried by the mean circulation (ii) waters expelled from the SJG, or (iii) water locally upwelled in SMG southern coast and advected northward by the mean circulation. In an attempt to clarify the possible physical mechanism in the ZF formation we conducted a series of additional process oriented numerical experiments (see Table 1). Only the January results, when the front is fully formed, are presented.

To test mechanism (i) we return to the NOTIDE experiment which did not form the surface pool of cold water, east of Valdés Península (Fig. 7b). Consequently, waters advected into the southern SMG are warmer than in the satellite data (Fig. 6d) and the benchmark experiment (BENCH, Fig. 7a). The surface currents are

Author's personal copy

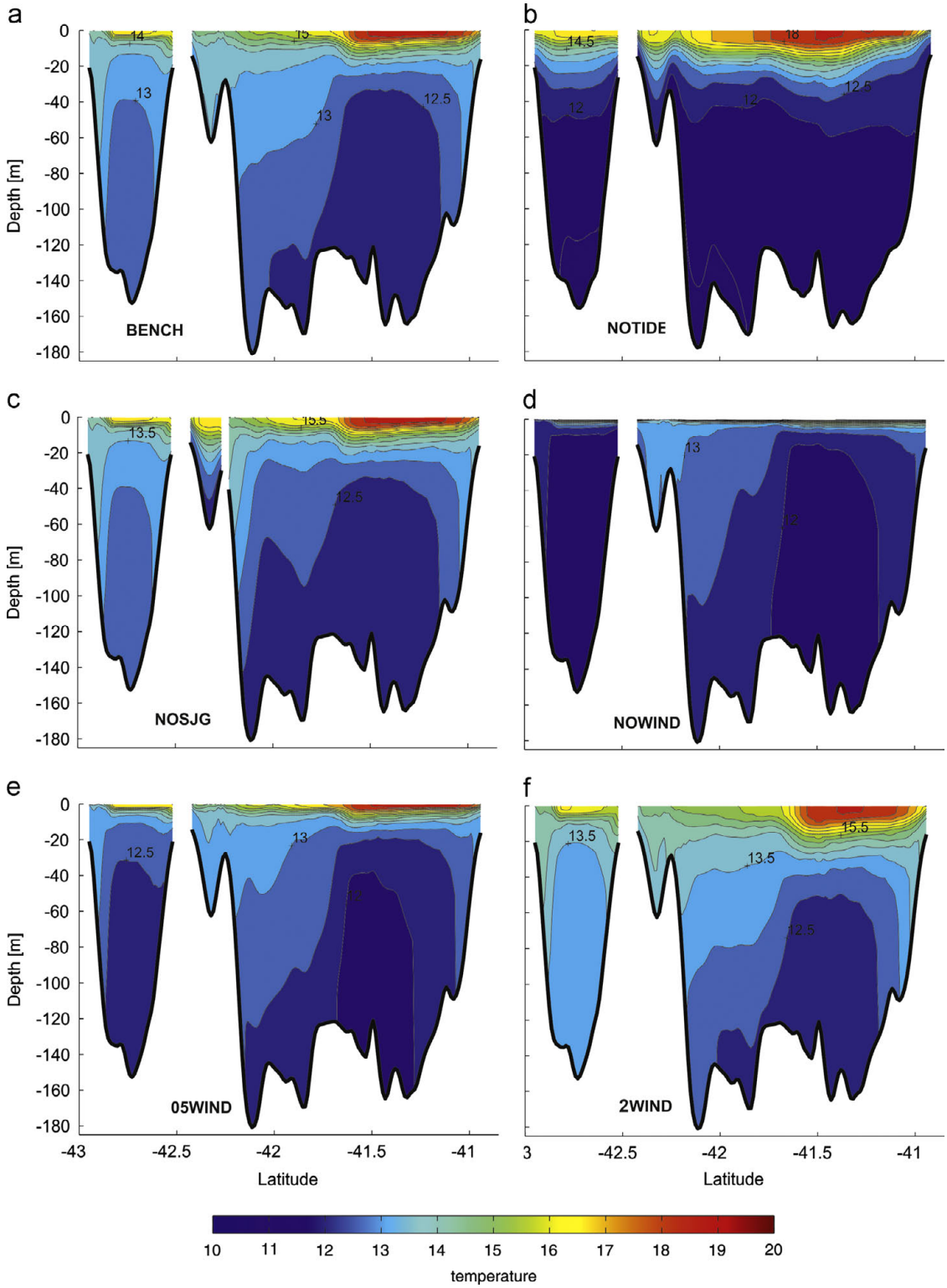

Fig. 8. Temperature cross-sections along line B (see Fig. 6c) in January (austral summer) (CI=0.5 °C). (a) Benchmark experiment (BENCH), (b) no tidal forcing at lateral boundaries (NOTIDE), (c) no connection between SMG and SJG (NOSJG), (d) no wind stress (NOWIND), (e) half wind stress magnitude (05WIND) and (f) double wind stress magnitude (2WIND).

weaker, therefore the transport is reduced. In the absence of vertical tidal mixing the southern and northern regions of SMG have similar stratification distributions (Fig. 8b) Thus, the bottom waters and the bulk of shelf waters below the mixed layer flowing into the gulf are colder than in experiments with tides (compare Fig. 8a and b). The region of relatively low surface temperature and the northward flow observed at the southern SMG coast suggests the influence of the southerly winds (Figs. 7b and 2a). In the NOTIDE simulation the meridional temperature gradient is weak and there is no indication of the presence of the ZF, as in BENCH (Fig. 9a).

To evaluate the role of waters expelled from SJG in the formation of the ZF we closed the gulf mouth (Experiment NOSJG). In this case the surface temperatures in the southern portion of

Author's personal copy

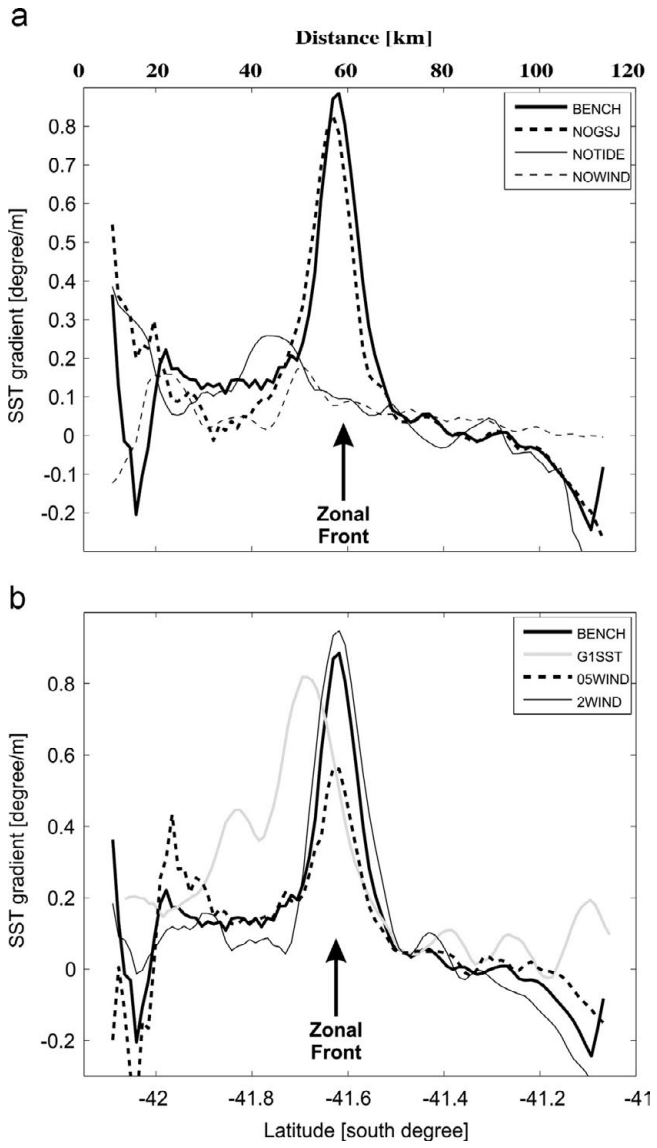

Fig. 9. January (austral summer) sea surface temperature gradients along line B. (a) BENCH, NOTIDE, NOSJG and NOWIND, and (b) sensitivity experiments to wind stress forcing, BENCH, 05WIND, 2WIND and satellite data G1SST.

SMG are slightly higher than in BENCH (Fig. 7c) and therefore the intensity of the ZF is reduced ~10% (Fig. 9a). The strong tidal mixing decreases and the stratification increases in the southern sector of SMG and inside SJG (Fig. 8c). The cold surface waters still observed in southern SMG appear to be due to the influence of waters from the western side of the VF that are advected by the surface circulation (Fig. 7c). Furthermore, when SJG is connected with SMG it is possible that a fraction of the VF waters re-circulate and mix inside SJG before being exported to SMG, as suggested by daily high resolution satellite images (Amoroso and Gagliardini, 2010). NOSJG shows that mixing through the mouth of SJG affects mainly the middle and deeper layers of the southern SMG (Fig. 8c) and therefore plays a secondary role in the formation of the ZF.

To test the role of the wind in the formation of the ZF, we conducted an additional experiment with the same settings as in BENCH but excluding wind stress forcing (NOWIND). Although this experiment forms the pool of cold water west of the VF (Fig. 7d) and tidal currents generate intense vertical mixing at the SJG mouth, in the absence of wind the advection of cold waters from the vertically mixed shelf regions into the southern sector of SMG is greatly reduced. The SST in SMG is practically uniform (Fig. 7d) and no ZF is formed (Fig. 9b). Additionally, without wind forcing, the weak coastal upwelling forced by the cross-shelf winds in experiment NOTIDE and suggested by the band of cold temperatures along the southeastern coast of SMG is suppressed and replaced by cold waters advected westward from the outer shelf (Figs. 7b and 7d). The absence of wind stress mixing decreases the vertical mixing of heat and the model develops a very thin and warm mixed layer overlaying the cold waters that occupy the bulk of the volume underneath (Fig. 8d). This experiment also shows that without wind forcing the tidal mixing between SJG and SMG only exerts a local influence on the SST in the southeast of the SMG and acts primarily to homogenize the deeper layers (Figs. 7 and 8d).

Due to uncertainties in the determination of the wind stress (algorithms used for processing the satellite data and parameterization of the turbulent exchange at the sea surface), and given its important role in determining the formation of the SMG ZF, we explore the response of the NPG to variations of the magnitude of the wind stress. Additionally, these experiments might be helpful to predict the frontal response under synoptic changes of the wind forcing. For this purpose we implemented two additional experiments: one forced with half the wind stress magnitude (05WIND), and the other doubling the wind stress magnitude (2WIND). The increase or decrease in the magnitude of wind stress modified mainly the depth of the thermocline in the northern half of SMG and the intensity of the SST gradient at the ZF, otherwise the SSTs structure and the frontal location are similar to BENCH. Halving the wind intensity (05WIND) reduced the thermocline depth (~7 m, Fig. 8e) and decreased more than 35% the intensity of the ZF (Fig. 9b). When we doubled the magnitude of the wind stress, the thermocline deepens from ~10 m in BENCH to ~20 m in 2WIND (Fig. 8f) and the SST gradient across the ZF is slightly increased (Fig. 9b). The intensity of the ZF in these experiments and the one estimated from the January 2011 SST observations are displayed in Fig. 9b. Though in the simulations the SST front is slightly south from its observed location, the frontal intensity compares well with the BENCH experiment.

3.5. The seasonal cycle

The summer circulation displays strong thermal fronts, robust gulf-wide gyres and intense re-circulations. Since these patterns can act as a retention mechanism of planktonic species (Brown et al., 1995; Hill et al., 1997) they may be important from a biological standpoint. Therefore, it is of interest to determine whether any of these patterns persist throughout the year, or show seasonal variability. To this end the seasonal cycle of the circulation is analyzed below based on the strength and structure of the vertically averaged stream function (Fig. 10 and 11). Vertically integrated patterns give us a more complete idea of the mean circulation and the impact of circulation structures discussed above.

In winter (July, Fig. 10a) the strong westerly winds (Fig. 2b) combined with the tidal residual circulation delineate a circulation pattern zonally dividing SMG and NG into two gyres of opposite sense of rotation. The western gyre is anticyclonic, while the eastern gyre is cyclonic (Fig. 10a). Further analysis of the NOTIDE and NOWIND experiments clearly shows that the cyclonic flow in the east is mostly driven by the tides (Fig. 10b) while the anticyclonic circulation in the west is sustained by the wind (Fig. 10c). The winter circulation pattern is very similar to that obtained by Tonini and Palma (2011) using a barotropic model and a spatially uniform (westerly) wind stress field.

In early spring (September, Fig. 11a) the wind stress intensity decreases and the heat flux begins to increase the water column stratification. In response to this change in the surface forcing

Author's personal copy

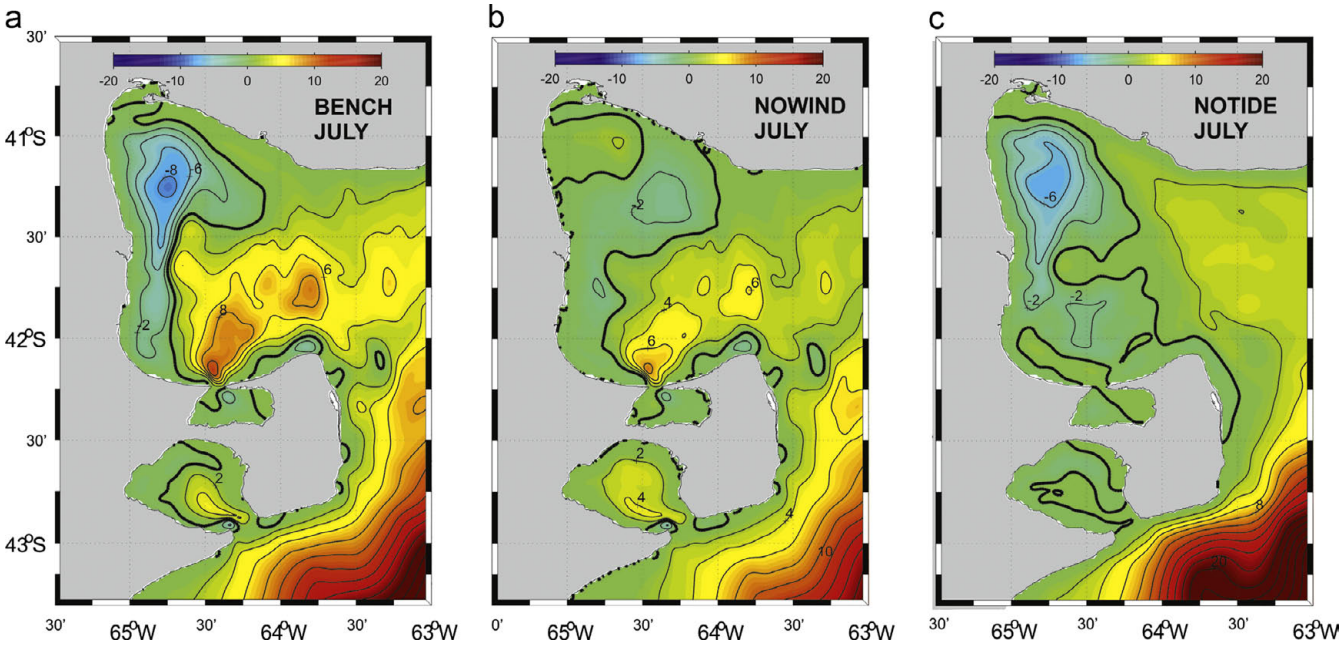

Fig. 10. July (austral winter) vertically integrated stream function (CI = 2 x 10^4 m^3/s). (a) BENCH, (b) NOWIND and (c) NOTIDE.

there is an intensification and expansion of the cyclonic circulation in the southern gyre of the SMG and the center of NG (Fig. 11a). The anticyclonic gyre, being mostly wind-driven, shrinks in size (Fig. 11a). By late spring (November, Fig. 11b) the evolving interaction of the stratification and the tidal forcing intensifies the southern cyclonic gyre and delineates a new re-circulating cyclonic subgyre in the northern half of SMG. A similar intensification of the circulation is observed in NG, but only a single cyclonic gyre is apparent (Fig. 11b).

In summer (January, Fig. 11c) the intensity of the two cyclonic subgyres in SMG reaches approximately 0.16 Sv, with the northern gyre being largest in size. The strongest cyclonic circulation in NG is also observed in this period (Fig. 11c). In late summer (March, Fig. 11d) the cyclonic gyres in SMG reach their highest intensity but begin to shrink in size. As a consequence of the summer's closed circulation patterns SMG and NG waters are more isolated from the shelf region.

The model results suggest that in autumn (May) the cyclonic circulation weakens in SMG and NG (Fig. 11e). Simultaneously a weak anticyclonic flow pattern develops along the west coasts of both gulfs. In SMG this flow is connected with two semi-permanents eddies located at the mouth of SJG. As the cyclonic circulation relaxes in fall and early winter the excess heat and salt accumulated in the northern part of SMG during the summer is exported to the neighboring shelf along the northern coast (Fig. 11e and f). The observation of high surface salinities (>34) in the inner shelf off the northern sector of SMG during this time of the year (Piola and Scasso, 1988; Lucas et al., 2005) suggests that the eastward flow from the gulf along the northern coast is the main export route of gulf waters to the adjacent continental shelf.

SJG shows a persistent year-long circulation pattern associated with the structure created by residual tidal currents at the mouth (a pair of counter-rotating eddies, Fig. 5b). Only the strong winds during winter appear to generate an anticyclonic gyre in the east coast (Fig. 11f).

4. Summary and conclusions

In the present study the mean three dimensional circulation of the NPG was explored with focus on the formation, interaction and seasonal variability of recirculation features (gulf-wide gyres and eddies) and frontal structures using a numerical model. The model was initialized with horizontally uniform temperature and salinity, was forced with monthly climatological winds, heat and salt fluxes at the surface and tides at the lateral open boundaries.

There are few direct current observations inside the gulf to validate the modeled flow pattern, but our results show that there is an intense cyclonic circulation in the northern SMG caused by the interaction of the tides and the evolving summer stratification in the presence of variable topography, and a smaller cyclonic subgyre in the south that seemed largely controlled by tidal residual currents. Similar circulation patterns in SMG had been previously inferred based on property distributions and the thermocline depth (Piola and Scasso, 1988). Cyclonic circulation patterns in the warmer upper layers of an enclosed shelf basin are also expected if there is a remnant dome of dense deep water that remains stagnant by the effect of increased tidal-induced bottom friction like in the SMG (Hill, 1996). The overall density structure displayed by the model in the central part of SMG is confirmed by in-situ observations. Similar circulation patterns associated with dense, stagnant bottom water lenses have been observed and modeled in the Middle Atlantic Bight (Houghton et al., 1982), the Adriatic Sea (Henderschott and Rizzoli, 1976), the Gulf of California (Lavin et al., 1997), the Yellow Sea (Hu et al., 1991), and Irish Sea (Hill et al., 1997).

The same physical mechanism seems responsible for the intensification of the summer cyclonic circulation in NG. This gulf has only one deep basin and therefore a single cyclonic gyre spanning the entire gulf is formed. The westward advection of cold waters, vertically mixed by the tides in the mouth region, contributes to the formation of a weak zonal surface front in summer clearly depicted in high resolution satellite derived SST distributions (Amoroso and Gagliardini, 2010). In contrast with SMG and NG, the SJG circulation appears to be relatively insensitive to the inclusion of surface heat flux forcing. The circulation at SJG is dominated by a pair of counter-rotating eddies generated by tidal residual currents near the mouth and extending towards the interior.

The model reproduced the observed patterns of the January SST distribution. Although the surface temperature range is larger than in the observations, both distributions present cold regions along

Author's personal copy

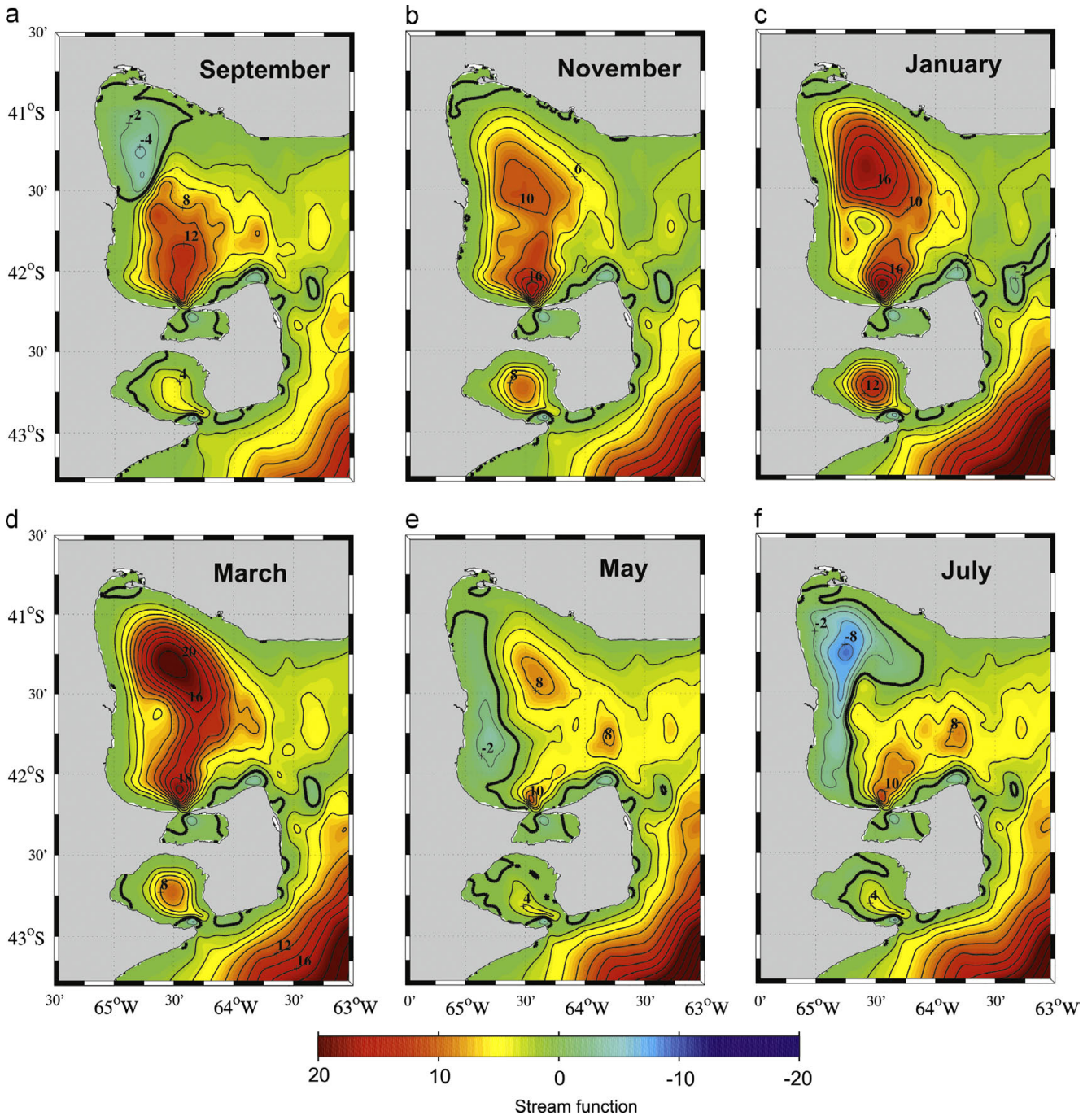

Fig. 11. Time evolution of the monthly mean vertically integrated stream function from the benchmark experiment (BENCH, CI = 2 x 10^4 m^3/s). Thick black lines indicate contours of null transport. (a) September, (b) November, (c) January, (d) March, (e) May and (f) July.

the mouths of SMG and NG and east of Valdés Península. The PEA distribution computed from the model results revealed the correct location of thermal fronts previously detected from remote sensing data, such as VF extending from Valdés Península in a SW–NE direction, a meridional front close to the SMG mouth and a zonal front dividing strongly stratified and weakly stratified waters within SMG. The model also captures a zonal temperature contrast inside SJG which has been described based on high resolution satellite data (Amoroso and Gagliardini, 2010). This feature is probably associated with the asymmetry in the location of the gulf's mouth, which leads to higher tidal mixing and homogenization in the west.

The modeled meridional contrast of SMG surface waters during summer (warmer and saltier (not shown) in the north; colder, fresher and less stratified in the south) is in overall agreement with hydrographic observations (Carreto et al., 1974; Piola and Scasso, 1988) and with estimates of the SST gradient based on satellite data (Rivas and Pisoni, 2010). A series of sensitivity experiments showed that the cold surface waters in the southern half of SMG are advected by the wind from the cold pool generated by intense tidal mixing east of Valdés Península. Without wind forcing the tidal mixing only exerts a local influence on the SST and acts primarily to homogenize the water column. Although it is possible that a fraction of the advected waters re-circulate and mix

Author's personal copy

inside SJG before being exported to SMG, as suggested by high resolution satellite images (Gagliardini and Rivas, 2004; Amoroso and Gagliardini, 2010), the experiments showed that mixing through the mouth of SJG affects mainly the mid and deeper layers of the adjacent SMG and therefore plays a secondary role in the formation of the ZF. Additional sensitivity experiments showed that variations in the wind intensity modified the depth of the thermocline in the northern half of SMG and the intensity of the SST gradient at the ZF, but otherwise the SST structure and the frontal location remains similar to the benchmark experiment.

The interaction of atmospheric (wind and heat fluxes) and tidal forcing drives a distinct seasonal circulation in the interior of SMG. In September the ocean begins to gain heat from the atmosphere and marks the spinup of a cyclonic circulation in northern SMG. By November, the gulf-scale cyclonic circulation pattern is established with two recirculation subgyres. The circulation accelerates throughout the summer and reaches its maximum strength in March. The fall-to-winter transition is characterized by decelerating cyclonic circulation and shrinking of the northern SMG subgyre and the appearance of an anticyclonic wind-induced gyre in the NW sector. The anticyclonic gyre grows in size with the intensification of the winter westerly winds, filling the entire western half of SMG and reaching its maximum meridional extension and strength in mid-winter (July–August). There is a similar seasonal response in NG, a single cyclonic gyre that intensifies in summer and shrinks in winter with the simultaneous developing of a weak anticyclonic circulation along the west coast. In contrast, the mean ocean circulation in SJG is dominated by a strong pair of counter-rotating eddies produced by tidal rectification year-round.

Monthly wind climatologies as those employed in this study are limited by the fact that the seasonal cycle contains a small percentage of the total wind variability in localized regions. A large part of this variability is concentrated in high-frequency scales (daily to weekly) associated with synoptic atmospheric variability. To the extent that the flow is only weakly non-linear, high frequency oscillations will probably have an impact on local and high-frequency circulations (like inertial oscillations) but no significant impact on the mean circulation patterns. Our weakly non-linear assumption is not only confirmed by the momentum balance of the model and observations (Piola and Scasso, 1988), which show that, to the zeroth-order, the gulf-wide circulation in SMG is in geostrophic balance, but also by the results of exploratory experiments (not shown) conducted with daily ERA Interim winds (Dee et al, 2011). The numerical solutions indicate limited high-frequency dependence in the time averaged ocean response, suggesting that the low-frequency response reflects the major features of the monthly mean circulation.

In summary, the numerical results showed that both tidal and wind forcing significantly contribute to delineate the frontal structures and the seasonal circulation in the NPG. The summer-mean circulation is mainly controlled by the interaction of the tides and the evolving stratification driven by surface heat and salt fluxes. The effects of wind forcing are more important in delineating the mean circulation in winter and in maintaining the SMG surface zonal thermal front in summer. The results derived from the numerical model are consistent with available data and represent a significant step forward in the understanding of the regional circulation.

Acknowledgments

MHT was supported by Postdoctoral Scholarship provided by CONICET, Argentina. Additional support was provided by Agencia Nacional de Promoción Científica y Tecnológica (ANCYPT-Grant PICT08-1874), CONICET (Grant PIP09-112-200801) and by Collaborative Research Network grant CRN2076 from the Inter-American Institute for Global Change Research, supported by the US National Science Foundation grant GEO-0452325. E. D. P. acknowledges partial support by Universidad Nacional del Sur (Grant F032). This paper benefited substantially from comments and suggestions given by the anonymous reviewers.

References

Acha, E.M., Mianzan, W.H., Guerrero, R.A., Favero, M., Bava, J., 2004. Marine fronts and the continental shelves of Austral South America, physical and ecological processes. Journal of Marine Systems 44, 83–105.

Amoroso, R.O., Gagliardini, D.A., 2010. Inferring complex hydrographic processes using remote-sensed images: turbulent fluxes in the patagonian gulfs and implications for scallop metapopulation dynamics. Journal of Coastal Research 26 (2), 320–332.

Amoroso, R.O., Parma, A.M., Orensanz, J.M., Gagliardini, D.A., 2011. Zooming the macroscope: medium-resolution remote sensing as a framework for the assessment of a small-scale fishery. Journal of Marine Science 68 (4), 696–706.

Barnier, B., 1998. Forcing the ocean. In: Chassingnet, E.P., Verron, J. (Eds.), Ocean Modelling and Parameterization. Kluwer Academic Publishers, The Netherlands, pp. 45–80.

Barros, V.R., Krepper, C.M., 1977. Modelo estacionario del Golfo Nuevo. Acta Oceanographica Argentina 1 (2), 11–29.

Bianchi, A.A., Ruiz-Pino, D., Isbert Perlender, H., Osiroff, A., Segura, V., Lutz, V., Luz Clara, M., Balestrini, C.F., Piola, A.R., 2009. Annual balance and seasonal variability of sea-air CO_2 fluxes in the Patagonia Sea: their relationship with fronts and chlorophyll distribution. Journal of Geophysical Research 114, C03018.

Bogazzi, E., Baldoni, A., Rivas, A., Martos, P., Reta, R., Orensanz, J.M., Lasta, M., Dell' Arciprete, P., Werner, F., 2005. Spatial correspondence between areas of concentration of Patagonian scallop (Zygochlamys patagonica) and frontal systems in the Southwestern Atlantic. Fisheries Oceanography 14 (5), 359–376.

Brown, J., Hill, A.E., Fernand, L., Bennett, D.B., Nichols, J.H., 1995. A Physical Retention Mechanism for Nephrops Norvegicus Larvae. ICES C.M. 1995/K:31 Ref. C (mimeo).

Carreto, J.I., Verona C.A., Casal, A.B., Laborde, M.A., 1974. Fitoplancton, Pigmentos y Condiciones Ecológicas del Golfo San Matías III. Instituto de Biología Marina de Mar del Plata, Informe N° 10, Contribución 237, CIC Pcia. de Buenos Aires, vol. 10, pp. 49–76.

Carreto, J.I., Bevídes, H., Negri, R., Glorioso, P.D., 1986. Toxic red tide in the Argentine Sea. Phytoplankton distribution and survival of the toxic dinoflagellate Gonyaulax excavata in a frontal area. Journal of Plankton Research 8, 15–28.

Conkright, M.E., Locarnini, R.A., Garcia, H.E., O Brien, T.D., Boyer, T.P., Stephens, C., Antonov, J.I., 2002. World Ocean Atlas 2001: Objective Analyses, Data Statistics, and Figures, CD-ROM Documentation. National Oceanographic Data Center. Silver Spring, MD p. 17.

daSilva, A., Young, A.C., Levitus, S., 1994. Atlas of Surface Marine Data 1994, Volume 1: Algorithms and Procedures. U.S. Department of Commerce, NOAA, NESDIS, Tech. Rep. 6.

Dee, D.P., Uppala, S.M., Simmons, A.J., Berrisford, P., Poli, P., Kobayashi, S., Andrae, U., Balmaseda, M.A., Balsamo, G., Bauer, P., Bechtold, P., Beljaars, A.C.M., van de Berg, L., Bidlot, J., Bormann, N., Delsol, C., Dragani, R., Fuentes, M., Geer, A.J., Haimberger, L., Healy, S.B., Hersbach, H., Hólm, E.V., Isaksen, L., Kallberg, P., Köhler, M., Matricardi, M., McNally, A.P., Monge-Sanz, B.M., Morcrette, J.-J., Park, B.-K., Peubey, C., de Rosnay, P., Tavolato, C., Thépaut, J.N., Vitart, F., 2011. The ERA-Interim reanalysis: configuration and performance of the data assimilation system. Quarterly Journal of the Royal Meteorological Society 137, 553–597.

Dickey-Collas, M., Brown, J., Fernand, L., Hill, A.E., Horsburgh, K.J., Garvine, R.W., 1997. Does the western Irish Sea gyre influence the distribution of juvenile fish? Journal of Fish Biology 51, 206–229.

Egbert, G.D., Bennett, A.F., Foreman, M.G., 1994. Topex/poseidon tides estimated using a global inverse model. Journal of Geophysical Research 99, 24821–24852.

Framiñan, M.B., Balestrini, C.F., Bianchi, A.A., Demilio, G., Piola, A.R., 1991. Datos CTD y Series Temporales de Velocidad, Temperatura y Conductividad en el Golfo San Matías. Servicio de Hidrografía Naval, Informe Técnico No. 63/1991, Argentina.

Gagliardini, D.A., Rivas, A.L., 2004. Environmental characteristics of San Matías Gulf obtained from LANDSAT–TM and ETM+data. Gayana (Concepción) 68 (2), 186–193.

Glorioso, P.D., 1987. Temperature distribution related to shelf-sea fronts on the Patagonian shelf. Continental Shelf Research 7 (1), 27–34.

Glorioso, P.D., Simpson, R.A., 1994. Numerical modelling of the M2 tide on the northern Patagonian shelf. Continental Shelf Research 14, 267–278.

Glorioso, P.D., Flather, R.A., 1997. The Patagonian Shelf tides. Progress in Oceanography 40, 263–283.

Haidvogel, D.B., Arango, H.G., Hedstrom, K., Beckmann, A., Malanotte-Rizzoli, P., Shchepetkin, A.F., 2000. Model evaluation experiments in the North Atlantic Basin: simulations in nonlinear terrain-following coordinates. Dynamics of Atmospheres and Oceans 32, 239–281.

Hill, A.E., 1996. Spin-down and the dynamics of dense pool gyres in shallow seas. Journal of Marine Research 54 (16), 471–486.

Author's personal copy

Hill, A.E., Brown, J., Fernand, L., 1996. The western Irish Sea gyre: a retention system for Norway Lobster (*Nephrops norvegicus*). Oceanologica Acta 19, 357–368.
Hill, A.E., Brown, J., Fernand, L., 1997. The summer gyre in the Western Irish Sea: shelf Sea paradigms and management implications. Estuarine, Coastal and Shelf Science 44 A, 83–95.
Henderschott, M.C., Rizzoli, P.M., 1976. The winter circulation of the Adriatic Sea. Deep-Sea Research 23, 353–370.
Horsburgh, K.J., Hill, A.E., Brown, J., Fernand, L., Garvine, R.W., Angelico, M.M.P., 2000. Seasonal evolution of the cold pool gyre in the western Irish Sea. Progress in Oceanography 46, 1–58.
Houghton, R.W., Schlitz, R., Beardsley, R.C., Butman, B., Chamberlin, J.L., 1982. The middle Atlantic Bight: evolution of the temperature structure during summer 1979. Journal of Physical Oceanography 12, 1019–1029.
Hu, D., Cui, M., Li, Y., Qu, T., 1991. On the Yellow Sea cold water mass related circulation. Yellow Sea Research 4, 79–88.
Lanfredi, N., Schmidt, S., Speroni, J., 1979. Cartas de corrientes de marea (Río de La Plata). IC-IT-79/03. Departamento de Oceanografía. Servicio de Hidrografía Naval, Buenos Aires p. 45.
Lasta, M.L., Bremec, C., 1998. Zygochlamys patagonica in the Argentine Sea: a new scallop fishery. Journal of Shellfish Research 17, 103–111.
Lavin, M.F., Durazo, R., Palacios, E., Argote, M.L., Carrillo, L., 1997. Lagrangian observations of the circulation in the Northern Gulf of California. Journal of Physical Oceanography 27, 2298–2305.
Lucas, A.J., Guerrero, R.A., Mianzan, M.W., Acha, E.M., Lasta, C.A., 2005. Coastal oceanographic regimes of the Northern Argentine continental shelf (34–43°S). Estuarine, Coastal and Shelf Science 65, 405–420.
Mazio, C.A., Dragani, W.C., Caviglia, F.J., Pousab, J.L., 2004. Tidal hydrodynamics in Golfo Nuevo, Argentina, and the adjacent continental shelf. Journal of Coastal Research 20 (4), 1000–1011.
Marchesiello, P., McWilliams, J.C., Shchepetkin, A., 2001. Open boundary conditions for long-term integration of regional oceanic models. Ocean Modelling 3, 1–20.
Marchesiello, P., McWilliams, J.C., Shchepetkin, A., 2003. Equilibrium structure and dynamics of the California current system. Journal of Physical Oceanography 33, 753–783.
Mellor, G.L., Yamada, T., 1982. Development of a turbulence closure model for geophysical fluid problems. Reviews of Geophysics and Space Physics 20, 851–875.
Moreira, D., Simionato, C.G., Dragani, W.C., Nuñez, M.N., 2009. Tidal and residual currents observations at San Matías and San José gulfs, Northen Patagonian, Argentina. Journal of Coastal Research 25 (4), 957–968.
Moreira, D., Simionato, C.G., Dragani, 2011. Modeling ocean tides and their energetics in the North Patagonia Gulfs of Argentina. Journal of Coastal Research 27, 87–102.
Palma, E.D., Matano, R.P., Piola, A.R., 2004a. Three dimensional barotropic response of the southwestern Atlantic shelf circulation to tidal and wind forcing. Journal of Geophysical Research 109, C08014, http://dx.doi.org/10.1029/2004JC002315.
Palma, E.D., Matano, R.P., Piola, A.R., Sitz, L.E., 2004b. A comparison of the circulation patterns over the southwestern Atlantic shelf driven by different wind climatologies. Geophysical Research Letters 31, L24303, http://dx.doi.org/10.1029/2004GL021068.
Piola, A.R., Scasso, L.M., 1988. Circulación en el Golfo San Matías. Geoacta 15 (1), 33–51.
Risien, C.M., Chelton, D.B., 2008. Global climatology of wind stress and wind stress derivative fields from 7 years of QuikSCAT scatterometer data. Journal of Physical Oceanography 38, 2379–2413.
Rivas, A.L., 1997. Current meter observations in the Argentine continental shelf. Continental Shelf Research 17, 391–406.
Rivas, A.L., Beier, E.J., 1990. Temperatura and salinity fields in the nortpatagonic gulfs. Oceanologica Acta 13, 15–20.
Rivas, A.L., Frank Langer, A., 1996. Mass and heat transport in the Argentine continental shelf. Continental Shelf Research 16, 1283–1285.
Rivas, A.J., Piola, A.R., 2002. Vertical stratification at the shelf off Northern Patagonia. Continental Shelf Research 22, 1549–1558.
Rivas, A., Pisoni, J.P., 2010. Identification, characteristics and seasonal evolution of surface thermal fronts in the Argentinean continental shelf. Journal of Marine Systems 79, 134–143.
Romero, S.L., Piola, A.R., Charo, M., García, C.E., 2006. Chlorophyll-a variability off Patagonia based on SeaWiFS data. Journal of Geophysical Research 111, C05021, http://dx.doi.org/10.1029/2005JC003244.
Robinson, I.S., 1983. Tidally induced residual flows. In: Johns, B. (Ed.), Physical Oceanography of Coastal and Shelf Seas. Elsevier, Amsterdam, pp. 321–356.
Sabatini, M., Martos, P., 2002. Mesozooplankton features in a frontal area off northern Patagonia (Argentina) during spring 1995 and 1998. Scientia Marina 66 (3), 215–232.
Scasso, L.M.L., Piola, A.R., 1988. Intercambio neto de agua entre el mar y la atmósfra en el Golfo San Matías. Geoacta 15 (1), 13–31.
Shchepetkin, A.F., McWilliams, J.C., 2005. The regional oceanic modeling system (ROMS): a split-explicit, free-surface, topography-following-coordinate oceanic model. Ocean Modelling 9, 347–404.
Simpson, J.H., 1981. The Shelf-sea fronts: implications of their existence and behavior. Philosophical Transactions of Royal Society of London A302, 531–546.
Tonini, M.H., Palma, E.D., 2011. Respuesta barotrópica de los Golfos Norpatagónicos Argentinos forzados por mareas y vientos. Latin American Journal of Aquatic Research 39 (3), 481–498.
Zimmerman, J.T.F., 1981. Dynamics, diffusion, and geomorphological significance of tidal residual eddies. Nature 290, 549–555.